Published in final edited form as:
J Neurochem. 2012 December ; 123(5): 700–715. doi:10.1111/jnc.12007.

Importance of cholesterol in dopamine transporter function

Kymry T. Jones[1], **Juan Zhen**[1], and **Maarten E.A. Reith**[1,2]

[1]Department of Psychiatry, New York University School of Medicine, New York, New York, USA

[2]Department of Pharmacology, New York University School of Medicine, New York, New York, USA

Abstract

The conformation and function of the dopamine transporter (DAT) can be affected by manipulating membrane cholesterol, yet there is no agreement as to the impact of cholesterol on the activity of lipid-raft localized DATs compared to non-raft DATs. Given the paucity of information regarding the impact of cholesterol on substrate *efflux* by the DAT, this study explores its influence on the kinetics of DAT-mediated DA efflux induced by dextroamphetamine, as measured by rotating disk electrode voltammetry (RDEV). Treatment with methyl-β-cyclodextrin (mβCD), which effectively depletes total membrane cholesterol- uniformly affecting cholesterol-DAT interactions in both raft and non-raft membrane domains- reduced both DA uptake and efflux rate. In contrast, disruption of raft localized DAT by cholesterol chelation with nystatin had no effect, arguing against a vital role for raft-localized DAT in substrate uptake or efflux. Supra-normal repletion of cholesterol depleted cells with the analogue desmosterol, a non-raft promoting sterol, was as effective as cholesterol itself in restoring transport rates. Further studies with Zn^{2+} and the conformationally-biased W84L DAT mutant supported the idea that cholesterol is important for maintaining the outward-facing DAT with normal rates of conformational interconversions. Collectively, these results point to a role for direct cholesterol-DAT interactions in regulating DAT function.

Keywords

cholesterol; dopamine efflux; nystatin; methyl-β-cyclodextrin; rotating disk electrode voltammetry

Introduction

An important regulatory component in maintaining dopamine homeostasis in the brain is the dopamine transporter (DAT), the primary target for psychostimulants like cocaine, methylphenidate and amphetamine. The DAT functions to clear extracellular dopamine (DA), thereby limiting DA lifetime after release (Rice and Cragg 2008). Altered DAT function—resulting in disturbed DA homeostasis—is implicated in drug addiction (Sulzer 2011;Russo *et al.* 2010;Dietz *et al.* 2009), eating disorders and obesity (Schoffelmeer *et al.* 2011;Speed *et al.* 2011;Zhen *et al.* 2006;Patterson *et al.* 1998) and Parkinson's disease (Kurian *et al.* 2011). Hence, greater understanding of the molecular mechanisms of the DAT—and how these mechanisms are altered in neuropsychiatric disorders—could provide insight into novel clinical treatments. In addition to translocation of DA from the extracellular to the intracellular space, the DAT can also operate 'in reverse' to *release*

[2]To whom correspondence and reprint requests should be addressed: Maarten E.A. Reith, New York University School of Medicine, 550 First Ave., New York, NY 10016. maarten.reith@med.nyu.edu.

The authors have no conflicts of interest to disclose.

intracellular DA, otherwise known as DAT-mediated efflux (Rothman *et al.* 2009). The physiological importance of reversed DA transport by the DAT has been highlighted in a recent review (Leviel 2011), pointing out many instances of relevance for this process. For example, endogenous glutamate in the substantia nigra affects DA transmission by excitatory membrane depolarization, promoting reversal of the DAT, in turn leading to DAT-mediated DA efflux which can be blocked by the selective DAT inhibitor GBR12909 and other potent DAT blockers (Falkenburger *et al.* 2001;Olivier *et al.* 1995). Reversed DA transport is also pharmacologically important in the action of the DAT substrate dextroamphetamine (AMPH) (see excellent review by (Sulzer *et al.* 2005)). Accordingly, AMPH as a substrate not only interferes with DA uptake by physically occupying the DAT (in lieu of DA itself), but also promotes DA efflux via reverse transport (Gnegy 2003;Sitte *et al.* 1998;Wall *et al.* 1995).

Previous studies have shown that the function of the DAT can be affected by manipulating membrane cholesterol levels. Depletion of membrane cholesterol with methyl-β-cyclodextrin (mβCD) was shown to lower both the DAT's affinity (K_m) for DA and its uptake velocity (V_{max}) in [^{3}H]DA uptake assays (Adkins *et al.* 2007; Cremona *et al.* 2011). Enhancement of cholesterol to supranormal values promoted an outward-facing conformation of the DAT, as demonstrated by enhanced accessibility of transporter cysteine residue sulfhydryl groups to a membrane-impermeant surface biotinylation reagent (Hong and Amara 2010). Although it is clear that cholesterol is an important component to lipid rafts (Allen *et al.* 2007;Pike 2006), there is no agreement as to whether these results indicate that the effects of cholesterol manipulation are due to direct interactions between cholesterol and the DAT in non-raft membrane regions (Cremona *et al.* 2011;Hong and Amara 2010) or are mediated by lipid-raft localized DATs (Foster *et al.* 2008;Adkins *et al.* 2007). Indeed, studies have shown the importance of cholesterol in maintaining ligand binding activity and function in other integral membrane bound proteins, including monoamine transporters (Liu *et al.* 2009;Magnani *et al.* 2004;Butchbach *et al.* 2004;Eroglu *et al.* 2002;Scanlon *et al.* 2001;Klein *et al.* 1995;Fernandez-Ballester *et al.* 1994). In the case of cholesterol and DAT, only one study has addressed the impact of cholesterol on *efflux* of DA. Cremona and colleagues showed that at positive membrane potential, AMPH-induced DA efflux is sensitive to depletion of flotillin-1, which is required to maintain localization of DAT in lipid rafts (Cremona *et al.* 2011).

We initiated this study to further explore the influence of cholesterol on DAT's functionality, with an emphasis on DAT-mediated DA efflux. To address the effects of cholesterol on DAT function, we applied radiotracer assays in conjunction with rotating disk electrode voltammetry (RDEV) to evaluate kinetic parameters of DAT in real time at a physiologically relevant temperature in HEK 293 cells stably expressing the human DAT. Treatment with methyl-β-cyclodextrin (mβCD) was used to effectively deplete cholesterol, impacting both lipid rafts and direct cholesterol-DAT interactions, while nystatin was used to sequester free cholesterol without altering total cholesterol availability—thereby mainly disrupting lipid rafts (Cremona *et al.* 2011;Pucadyil *et al.* 2004;Simons and Toomre 2000;Rothberg *et al.* 1990). To assess sterol specificity, repletion of cholesterol deprived cells with desmosterol, a non-raft promoting sterol (Vainio *et al.* 2006), was employed in addition to repletion with cholesterol itself. Further studies with Zn^{2+} (which binds to the extracellular face of the DAT and promotes an open-to-out transporter conformation) and conformationally-biased W84L DAT were performed in order to examine the effects of cholesterol manipulation on DAT's conformational states. Our major findings demonstrate the importance of direct cholesterol (sterol)-DAT interactions in regulating transporter function.

Materials and Methods

Chemicals and solutions

Reagents were purchased as follows: [^{3}H]dopamine (34.6 Ci/mmol) and [^{3}H]CFT (76.0 Ci/mmole) were from Perkin-Elmer (St. Louis, MO). Dulbecco's Modified Eagle's Medium F12 (DMEM), Dulbecco's phosphate buffered saline (DPBS), Minimum Essential Medium Eagle (MEM), Brij 58, dopamine (DA), cocaine, dextroamphetamine ((+)-AMPH), cholesterol (CHOL), desmosterol (DESMO), nystatin, and methyl-β-cyclodextrin (mβCD) were from Sigma-Aldrich (St. Louis, MO). Unlabeled β-CFT was from the National Institute of Drug Abuse (Research Triangle Institute, Research Triangle Park, NC). Penicillin/streptomycin, fetal bovine serum, fetal calf serum, glutamine and all reagent grade cell culture chemicals were from Fisher scientific (Fair Lawn, NJ). The DC protein assay kit was from Bio-Rad (Hercules, CA).

Cell culture and preparation

Human Embroynic kidney cells (HEK 293) stably expressing the human dopamine transporter (HEK 293-hDAT (DAT WT)) or W84L DAT mutant (W84L) were maintained in DMEM-F12 (Chen *et al.* 2004b;Chen *et al.* 2001). Media were supplemented with 5% fetal bovine serum (FBS), 5% bovine calf serum (Hyclone, Logan, UT), 2mM glutamine, 200 μg/ml geneticin (G418), 100 IU /mL penicillin, and 100 μg/mL streptomycin. Pig kidney epithelial cells (LLC-PK) stably expressing human DAT (LLC-PK-hDAT) were cultured in MEM supplemented with 10% FBS, 2 mM glutamine, and 200 ug/mL G418. All mycoplasma free cells were maintained at 37°C with 5% CO_2. LLC-PK cells were a gift from Dr. Roxanne Vaughan (the University of North Dakota, Grand Forks, ND). Confluent cells were rinsed once with warm 1X PBS and subjected to various treatments in serum free DMEM (SF-DMEM) for the allotted times at 37°C. Cells were then trypsinized, spun down at 1,000 × g for 2 min, washed once with warm 1X PBS, and resuspended in appropriate buffer.

Preparation of cholesterol and desmosterol

Cholesterol and desmosterol were dissolved in 1:1 methanol:chloroform, dried with N_2, and stored at −20°C until use. Dried desmosterol and cholesterol were precomplexed with 2.5mM mβCD prior to use by adding 10 ml of SF-DMEM, sonicated for 10 seconds, and incubated overnight in a shaker at 37°C (Christian *et al.* 1997). Cholesterol depleted cells were repleted with either cholesterol or desmosterol complexed with mβCD by incubating for 2 hrs at 37°C with an mβCD/sterol complex (molar ratio 12.5:1) at a final sterol concentration of 200 μM.

Cholesterol quantification

Cell suspensions were placed in lysis buffer (1:5) provided by the Amplex Red Cholesterol kit (Invitrogen, Carlsbad, CA) and stored at −20°C. Analysis was performed in the absence of cholesterol esterase to detect unesterified cholesterol according to the manufacturer's protocol.

Preparation of cell lysates and surface biotinylation

In 10cm dish, treated cells were gently rinsed three times with ice cold DPBS containing 1 mM $MgCl_2$ and 0.1 mM $CaCl_2$ ($DPBS^{CM+}$, pH7.4) and incubated with 0.3 mg/ml SulfoLink NHS-SS-biotin (Thermo Scientific, Rockford, IL) in chilled $DPBS^{CM+}$ for 30 min at 4°C. Reactions were terminated by washing cells two times with ice-cold 100 mM glycine and incubated for 10 min at 4°C followed by additional washes (3Xs) in cold DPBS. Cells were lysed in 1% Brij buffer (1% Brij in Krebs/Ringer/HEPES lysis buffer (KRH) supplemented

with protease inhibitors (PI)) for 30 min on ice and further solubilized by passing lysates through a 22 gauge needle. Lysed samples were spun down at 1,200 × g for 10 min at 4°C. Supernatants were analyzed for protein content using DC protein assay. Cell lysates (200 μg) were added to 100 μl of NeutrAvidin Agarose Resin (Thermo Scientific) and incubated at ambient temperature for 2 hours with end-over-end mixing. Columns were washed 3Xs with 0.1% Brij buffer and bound biotinylated proteins were eluted with 70 μl of 2X elution buffer (125 mM Tris, pH 6.8, 2% SDS, 20% glycerol) supplemented with 25 mM dithiothreitol at 37°C for 50 min. Total lysates were mixed with 4X NuPAGE loading buffer containing reducing agent (Invitrogen). Total and surface biotinylated proteins were heated at 65°C for 10 min and loaded onto 4–12% Bis-Tris gels (Invitrogen) for separation by SDS-PAGE. Western blots were probed using anti-rat DAT (Millipore, Temecula, CA; 1:1000) and anti-rabbit actin antibody (Millipore; 1:2000). The amount of DAT surface expression was assessed by determining the relative ratio of biotinylated DAT to total hDAT normalized to actin levels for each treatment. Changes in DAT surface band densities were expressed as the percentage of control

Sucrose density fractionation

Equal amounts of protein (0.5–1.0 mg/ml) were equalized in volume and added to 80% (w/v) sucrose and mixed thoroughly in a 1:1 ratio. Samples in 40% sucrose were overlaid successively with 0.85 mls of 30% and 15% sucrose and 0.65 mls of 5% sucrose (in 1% Brij buffer + PI) in an ultracentrifuge tube. Samples were centrifuged at 217,000 × g for 20 hrs (4°C) using a Sorvall WX ultra series centrifuge (Thermo Scientific; TH-660 rotor). Fractions (0.33 ml) were collected from the top and aliquots were processed for SDS-PAGE and immunoblotting using anti-rat DAT, anti-mouse flotillin-1 (BD Transduction Laboratories, San Jose, CA; 1:1000) and anti-mouse Transferrin receptor (TfR) antibodies (Invitrogen; 1:1000).

Immunoblot analysis

Secondary antibodies conjugated to horseradish peroxidase were obtained from Pierce (Rockford, IL) and used at 1:5000 dilution. Blots were developed with Supersignal West Femto chemiluminescent substrate (Thermo Scientific) and visualized using the Odyssey Infrared Imaging System (Li-Cor, Lincoln, NE). Images acquired were analyzed using ImageJ 1.46i (NIH, USA) to obtain integrated densities.

Measurement of [^{3}H]DA uptake and [^{3}H]CFT binding and DA competition with CFT

For both binding, competition and uptake assays, suspensions of intact HEK 293-hDAT cells were prepared according to our previously reported procedures (Schmitt *et al.* 2008;Chen *et al.* 2001). Cell slurry was resuspended in 1.7 mls modified Krebs/Ringer/HEPES (KRH) buffer containing 1 mM ascorbic acid and 0.1 mM tropolone and used within 15 minutes. Assays were conducted in 96-well plates at 25°C, with all determinations performed in triplicate. Competition and binding assays was initiated by addition of 20 μl cell suspension to buffer containing 3–5 nM [^{3}H]CFT and varying concentrations of unlabeled DA at final concentration ranging from 0.3 μM-0.1 mM or unlabeled β-CFT at a final concentration ranging from 1.0 nM-0.3 μM for a final per-well reaction volume of 200 μl containing vehicle, mβCD, or nysatin. Nonspecific binding was determined with 1.0 μM unlabeled CFT.

Uptake was initiated by incubating cell suspensions with varying concentrations of non-radiolabeled DA (1.0 nM-100 μM) along with 6–10 nM [^{3}H]DA for 5 minutes at room temperature. Nonspecific uptake was determined using 10 μM cocaine. [^{3}H]CFT binding and [^{3}H]DA uptake assays were terminated by cold, rapid vacuum filtration onto a Wallac B filtermats using a Brandel 96-pin manual harvester. All assays were performed in triplicate

and expressed as mean ± SE calculated using Biosoft Kell Radlig software (Cambridge, UK). Tritium accumulation was quantified using a microbeta 1405 liquid scintillation counter. Total radioligand added was assessed using a LS 6500 Multi-Purpose Scintillation Counter, Beckman Coulter, Inc (Fullerton, CA. USA). Dpm per well was converted to pmoles and then corrected to mg of total protein per well.

Measurement of DA uptake and efflux with Rotating Disk Electrode Voltammetry (RDEV)

HEK 293 cells stably expressing hDAT (WT) or W84L were cultured to confluence and other general methods were as we described previously (Chen and Justice 2000;Chen *et al.* 1998). Treated cells were harvested by trypsinization, washed with 1X PBS, and resuspended in 1.2 mls of assay buffer (120 mM NaCl, 4.7 mM KCI, 2.2 mM $CaCI_2$, 1.2 mM $MgSO_4$, 1.2 mM KH_2PO_4, 10 mM HEPES, and 10 mM glucose (pH 7.4)) with or without compounds. Resuspended cells were kept at 37°C for no longer than 40 minutes and diluted 1:2 in assay buffer before use. Cells suspensions (300 μL) were added to the electrochemical chamber (37°C) with a rotating working electrode (at 4000 rpm). The oxidized DA current (+0.4 V vs. Ag/AgCl reference electrode) was recorded every 300 ms by a National Instruments (Austin, TX) PC interface board. After one minute of baseline signal acquisition, final concentrations of dopamine ranging from 0.15–7.5 μM were added to cell suspension to initiate the uptake measurement. For zinc experiments, 30 μM Zn^{2+} was added for one minute prior to dopamine addition. Once the oxidized DA current was cleared to a plateau close to baseline, dextroamphetamine ((+)-AMPH) was added at a final concentration of 10 μM to induce DA efflux. Recording was continual until no increase of oxidized DA current was observed, *i.e.* an elevated plateau was reached. The electrochemical chamber was washed 5 times with water before carrying out the next assay. Protein level in each assay was determined by the DC protein method. Initial DA uptake and efflux rates (pmol/sec/mg) were calculated with the Origin Labtalk program at each tested DA concentration. Kinetic parameters (K_m and V_{max}) of uptake and efflux were estimated by nonlinear fitting of the initial uptake or efflux rate to the initial added concentration of DA according to the Michaelis-Menten equation for saturation (linearly represented by the Scatchard equation) using the Biosoft Kell Radlig software. Results of 4–12 independent experiments were expressed as mean ± SE. Graphpad Prism 5 was used to represent raw data in graphical form applying the Michaelis-Menten equation to the averaged data for each separate DA concentration as part of the DA concentration curve. For statistical analysis, the K_m and V_{max} values obtained per separate experiment by the above Kell analysis were used. To address DA release efficiency, the efflux and uptake V_{max} were expressed as a ratio for each independent experiment. These ratios were used for statistical analysis and calculation of group averages. It is important to point out that the latter average is not necessarily identical to the ratio of the average efflux V_{max} over uptake V_{max}.

Measurement of [^{3}H]DA efflux

LLC-PK-hDAT cells were grown in 24-wells plates to 90% confluency. Cells were quickly washed with prewarmed KRH assay buffer (RDEV buffer) followed by a 20 minute incubation at 37°C with or without compounds. Cells were incubated with equal amounts of [^{3}H]DA for an additional 20 minutes at 37°C. Plates were retrieved and quickly washed with ice-cold PBS (3Xs) followed by addition of assay buffer (200 μL) containing vehicle or 10 μM AMPH to corresponding wells. To ensure treatment effects, vehicle, mβCD, or nystatin were present in the assay efflux buffer. After a 5 minute incubation at 25°C, [^{3}H]DA released into supernatant was assessed by Wallac Trilux liquid scintillation counter. [^{3}H]DA efflux in the absence and presence of AMPH represented basal and induced efflux, respectively. Results are expressed as AMPH-induced release as a percentage of basal [^{3}H]DA levels for individual treatments performed in duplicate. To assess [^{3}H]DA incorporated, separate cells were washed with cold PBS (3Xs), precipitated with 5% ice-

cold trichloroacetic acid (TCA) for 30 minutes at 4°C, and measured by liquid scintillation counting.

Statistical analysis

The threshold for significance employed throughout was $P < 0.05$, and significance values were calculated by one-way ANOVA with appropriate *post hoc* tests using SigmaStat Version 3.5 (Ashburn, VA). Where appropriate for equality of standard deviations of multiple groups to be compared, values were log transformed prior to ANOVA.

Results

Effect of cholesterol manipulation on level of cholesterol in cells

In this work, we aimed for lowering the level of unesterified cholesterol in cells by treating DAT expressing HEK-293 cells at 37°C with the cholesterol depleting agent methyl-β-cyclodextrin (mβCD) (2.5 or 5.0 mM) for 30 min as in the work by Foster *et al.* (2008). Indeed, both concentrations significantly reduced cholesterol content compared with untreated cells by 39 or 63%, respectively (Fig. 1). Repletion was achieved by incubating 5.0 mM mβCD (30 min) treated cells with 200 μM cholesterol or desmosterol (precomplexed with mβCD) at 37°C for 2 hrs. Cholesterol content after sterol exchange was increased by 108 or 65%, respectively, over starting values. In contrast, nystatin (25 μg/ml) —a polyene antifungal agent that, in low doses, acts as a chelator of free cholesterol—is able to maintain cholesterol in cell membranes (Cremona *et al.* 2011) and indeed, did not change the overall content of cholesterol in our cells (Fig. 1).

Effect of cholesterol manipulation on lipid raft localization

Treatment with mβCD removes membrane cholesterol and increases membrane fluidity, which thereby interferes with both lipid raft formation (including proteins and lipids therein) and specific cholesterol-protein interactions in non-raft regions (Zidovetzki and Levitan 2007). In contrast, nystatin sequesters rather than extracts membrane-bound cholesterol (Sorkina *et al.* 2005;Jayanthi *et al.* 2004) and therefore impedes lipid raft formation by decreasing local concentrations of cholesterol (Cremona *et al.* 2011). In order to confirm, under our conditions, that nystatin shifts the subcellular distribution of DAT away from rafts, as does mβCD, treated cells were solubilized in 1% Brij and subjected to fractionation in a discontinuous sucrose density gradient by ultracentrifugation. Western blot analysis of 12 fractions revealed that the DAT under control conditions was distributed in a bimodal fashion with the majority found in regions of the gradient containing lipid rafts (fractions 3–5) and to a lesser extent in non-raft regions (Fractions 8–12) (Fig. 2). Nystatin, as well as mβCD, induced a significant shift of DAT out of raft fractions 3–4 into denser fractions 7 and up as can be seen in representative blots (Fig. 2A) and confirmed by quantification of all experiments (Fig. 2B). Repletion of mβCD depleted cells with cholesterol restored DAT association with low buoyant density fractions indicating reformation of DAT containing rafts (Fig. 2A and C). However, repletion with desmosterol, a non-raft promoting sterol, was inefficient at restoring rafts and thereby DAT remained primarily in the denser gradient fractions as seen with mβCD alone (Fig. 2A and C). The results support the use of nystatin as a raft disrupting agent under the conditions of the present experiments, in agreement with the sucrose gradient data for nystatin from Cremona *et al.* (2011), as well as lipid raft disruption by mβCD. Moreover, the data are consonant with the idea that repletion with cholesterol, but not desmosterol, allows the reformation of lipid rafts. Further analysis revealed that the gradient profile for the raft marker flotillin-1 resembled more, and the non-raft marker transferrin receptor (TfR) less, that of DAT (see Supplementary Information).

Effect of cholesterol manipulation on [^{3}H]DA uptake, [^{3}H]CFT binding, and DAT surface expression

Desorption of membrane cholesterol by 5.0 mM mβCD reduced the V_{max} and K_m of DA uptake as measured by tracer [^{3}H]DA assays (Table 1). Replenishment of cholesterol to mβCD treated cells restored the V_{max} and K_m towards control cells. In contrast to the effects of reduced cholesterol on DAT substrate uptake kinetics (V_{max}), there were no significant changes observed in inhibitor binding kinetics. That is, cholesterol manipulation did not alter the absolute binding affinity (K_d) of the cocaine analogue [^{3}H]CFT in intact HEK-hDAT cells. However, the K_i of DA in inhibiting [^{3}H]CFT binding was 1.5-fold lower (*i.e.* increased affinity) in cholesterol depleted cells than untreated cells, consonant with the mβCD-induced reduction in K_m for [^{3}H]DA uptake, a measure in part determined by the K_i of DA binding (Erreger *et al.* 2008;Chen *et al.* 2001;Zhang *et al.* 1997).

Cholesterol manipulation did not alter the maximum number of binding sites (B_{max}) for [^{3}H]CFT in intact HEK-hDAT cells, an assay that mostly reflects surface DAT (Chen and Reith 2004). To address more directly the impact of cholesterol on surface DAT, we performed surface biotinylation assays in stably expressing HEK-293 hDAT cells. Western blot analysis revealed no significant changes in the levels of DAT after treatment with mβCD, nystatin, or repletion with cholesterol or desmosterol (Fig. 3). This was true for both DAT in total lysates (representative blots, Fig. 3A, right) and the biotinylated surface fraction (Fig. 3A, left). Quantification of DAT surface expression (Fig. 3B) showed no significant effect by any treatment, arguing against internalized DAT as a plausible explanation for observed decreases in DAT function.

Effect of cholesterol manipulation on DA uptake and efflux as measured by RDEV

In addition to the classical radioligand binding and uptake assays, we also used rotating disk electrode voltammetry (RDEV) *in vitro* to assess real time changes in DAT activity. Consistent with our radiotracer assays, we found a reduced K_m and V_{max} of DA uptake following 5.0 mM mβCD treatment, with more control-like values upon cholesterol restoration (Fig. 4A). In contrast, nystatin (25 μg/ml) had no significant effect on DA uptake (Fig. 4A). Because this reagent impedes lipid raft formation by decreasing local concentrations of cholesterol (see above), the lack of effect suggests raft-localized DAT are not critical in DA uptake. In support, repletion with desmosterol, the cholesterol precursor which differs from cholesterol only in the presence of one double bond in the aliphatic chain (Stevenson and Brown 2009), restored uptake values towards control levels, as did cholesterol itself (Fig. 4A). The biophysical properties of desmosterol fail to form and maintain lipid rafts, in direct opposition to cholesterol (Singh *et al.* 2009;Vainio *et al.* 2006), consonant with our sucrose gradient data (Fig. 2); thus, the repletion data, along with the lack of appreciable nystatin effect, argues against a considerable role of raft-localized DAT in DA uptake functionality. Rather, the results indicate an important direct effect of sterol/cholesterol on DA uptake.

Within the same cell suspension, once accumulated DA reached plateau levels (with medium DA back to baseline), 10 μM of AMPH was as added to induce transport reversal. RDEV measurements showed a large reduction by mβCD in the K_m and V_{max} of AMPH-induced DA efflux while nystatin treatment had no effect (Fig. 4B). It should be kept in mind that AMPH needs to be taken up in order to promote DA efflux because in this system, AMPH-induced DA efflux as measured by RDEV is primarily exchange-based (Chen *et al.* 1998). Correction for the uptake velocity of AMPH was incorporated in the ratio of efflux V_{max} / uptake V_{max} for each independent experiment and then averaged ("corrected efflux V_{max}"); the latter is not necessarily identical to the ratio of the average efflux V_{max} over uptake V_{max}. One finds a residual reduction in corrected efflux V_{max} by mβCD at 37°C—

from 1.6 (control) to 0.9 (5.0 mM mβCD), a ~40% reduction in reverse transport (Fig. 4C). The corrected efflux V_{max} became indistinguishable from control values upon repletion with either cholesterol or desmosterol. Importantly, nystatin treatment showed no significant change in the corrected efflux V_{max} (Fig. 4C). As uptake, efflux appears to depend more on direct interactions between the DAT and cholesterol/sterol than on raft-localized DAT.

Effect of cholesterol manipulation on DA efflux as measured by retention of preloaded [^{3}H]DA

We also monitored DA efflux by a more classical approach. For this purpose, we measured the loss of preloaded [^{3}H]DA induced by AMPH in LLC-PK cells stably expressing hDAT, which were chosen for their robust attachment to culture dishes and resilience to extensive washing (in contrast to the less firmly attaching HEK cells). Addition of 10 μM AMPH to LLC-PK-hDAT cells produced an increase in [^{3}H]DA efflux to a level ~144% over basal efflux (Fig. 5). Treatment with 2.5 and 5.0 mM mβCD reduced [^{3}H]DA efflux to a value of 122 and 115%, respectively, over basal levels, representing a ~20% loss in efflux function. However, AMPH-induced DA efflux was unaffected by nystatin (150% versus 144% for control cells). Thus, as was observed for DA efflux with RDEV in HEK 293-hDAT cells, efflux of [^{3}H]DA in LLC-PK-hDAT cells was susceptible to mβCD but not to nystatin (Fig. 5).

Effect of manipulation of DAT conformational state with Zn^{2+} before and after cholesterol depletion on DAT function

Cholesterol has been reported to be important for maintaining the DAT in an outward-facing conformation (Hong and Amara 2010). We therefore reasoned that loss of cholesterol-DAT interaction may lower the fraction of DAT in an outward-facing conformation. In that case, Zn^{2+}, which is known to stabilize the outward-facing conformation (Liang *et al.* 2009;Schmitt *et al.* 2008;Loland *et al.* 2004;Chen *et al.* 2004a;Norregaard *et al.* 1998) should have a favorable effect in restoring DAT function under low cholesterol conditions. To test this, HEK-hDAT cells in the presence or absence of 2.5 mM mβCD were subjected to RDEV recordings with or without 30 μM Zn^{2+} for 1 minute prior to DA addition. In the absence of Zn^{2+}, 2.5 mM mβCD had an effect on DA uptake and AMPH-induced efflux that was similar to 5.0 mM mβCD (compare Fig. 6A with Fig. 4A). The observation that both uptake and efflux (induced by AMPH) were compromised by mβCD (with a reduction in both V_{max} and K_m) is reminiscent of the properties observed for T62A hDAT by Guptaroy *et al.* (2009). The behavior of this mutant was interpreted as reflecting a slower than normal transition between inward- and outward-facing conformations. Therefore we propose that mβCD-treated DAT resembles T62A hDAT in that such in-out transitions are slowed. When mβCD-treated cells were preincubated with Zn^{2+}, there was no statistically significant effect of Zn^{2+} on the uptake V_{max} (Fig. 6A) whereas the efflux V_{max} was increased to control values (Fig. 6B); the latter when corrected for uptake was fully restored to control levels (Fig. 6C). It should be considered here that Zn^{2+} by itself in otherwise untreated cells impedes uptake (Fig. 6A), as reported previously (Bjorklund *et al.* 2007;Chen *et al.* 2004a;Loland *et al.* 2002;Norregaard *et al.* 1998), in part by Zn^{2+} hindering conformational changes needed for substrate translocation (but see also (Scholze *et al.* 2002)). Stabilization of outward conformations by Zn^{2+} explains the efflux enhancement towards control values (opposite to efflux reduction seen with AMPH as efflux inducer in DAT mutants with an inward bias such as D345N (Chen *et al.* 2004a) and T62D (Guptaroy *et al.* 2009). Please note here that Zn^{2+} by itself did not affect the efflux V_{max} ratio (Fig. 6C). In the case of DA uptake, it is not clear why Zn^{2+} treatment of mβCD-treated cells (resulting in a V_{max} of 29.7 pmol s^{-1} mg^{-1}, Fig. 6A) did not further reduce the V_{max} to levels observed in cells treated with Zn^{2+} only (11.9 pmol s^{-1} mg^{-1}, Fig. 6A).

Manipulation of conformational state of the DAT by W84L mutation and impact of cholesterol on DAT function

Efforts in our laboratory have revealed that the W84L mutant prefers an outward-facing conformation and as a result DA uptake is inhibited (Chen *et al.* 2004b;Chen and Reith 2003). Because of the work linking cholesterol action on DAT with transporter conformations (Hong and Amara 2010), we employed the use of the outward-facing W84L hDAT mutant as a tool. Treatment with 2.5 mM mβCD partially restored the inhibiting effect of the W84L mutation on [^{3}H]DA uptake by increasing its V_{max} towards that of DAT WT, without a significant change in uptake K_m (Table 2). Furthermore, experiments on DA inhibition of [^{3}H]CFT binding showed mβCD treatment restored DA affinity (K_i) for the W84L mutant to a value similar to that observed in HEK 293-hDAT cells (Table 2). As we reported previously (Liang *et al.* 2009), CFT affinity (K_d) in W84L DAT was substantially lower than in DAT WT, and as expected cholesterol desorption with mβCD had no effect on CFT affinity (K_d) or maximal binding sites (B_{max}) in the W84L mutant as shown in Table 2. Further analysis revealed that the V_{max} / B_{max} turnover rate, a measure of DA uptake efficiency per minute (Bonisch 1998) was calculated to be 0.98±0.15 (mean ± SE) for DAT WT, 0.46±0.11 for W84L mutant, and 0. 71±0.14 for W84L±2.5mM mβCD (values in the absence of mβCD agree with our earlier data (Chen and Reith 2003)). The data suggest that cholesterol depletion can result in ~25% recovery in W84L DAT-mediated DA turnover.

Further studies with RDEV revealed similar findings for radiotracer assays performed with the W84L mutant. Treatment with 2.5 mM mβCD enhanced uptake V_{max} without altering K_m (Fig. 7A). Importantly, nystatin (25 μg/ml) did not significantly change V_{max} or K_m, suggesting raft localization of W84L DAT is not important for DA uptake functionality, just as raft disruption leaves uptake by DAT WT largely intact. AMPH-induced DA efflux showed a similar pattern as uptake indicated by a partial rescue of efflux V_{max} by mβCD without a change in K_m (Fig. 7B). The V_{max} ratio (incorporating the uptake correction) in mβCD treated W84L cells was rescued to that of DAT WT control (Fig. 7C). Again, nystatin did not affect efflux K_m, V_{max}, or V_{max} ratio (Fig. 7), arguing against the importance of lipid raft-localized W84L DAT for uptake and efflux functionality.

The partial functional rescue observed with mβCD treatment of the W84L mutant is consonant with the idea that cholesterol removal counteracts the conformational outward bias of W84L hDAT by removing the effect of cholesterol in promoting outward conformations of DAT (Hong and Amara 2010). However, the evidence provided by the W84L mutant is weak because the restoration, especially that of uptake function, was only partial (V_{max} of 10.16 pmol s^{-1} mg^{-1} rescued to 15.78 pmol s^{-1} mg^{-1}, Fig. 7A, compared with a WT V_{max} of 76.11 pmol s^{-1} mg^{-1}, Fig. 6A). Two caveats need to be considered here. First, it is unknown how far along the scale of outward to inward mβCD has impacted the conformation of W84L. In the extreme, mβCD could have fully induced an inward state as observed for mβCD-treated which was observed to have only a V_{max} of 23.12 pmol s^{-1} mg^{-1} (Fig. 6A). Second, as inferred from the experiments presented in the previous subsection, mβCD also slows down the transitions between inward- and outward-facing conformations. The results from this and the previous section, along with the work of Hong and Amara (2010), suggest that cholesterol removal slows down the conversion from out- to in-states slightly less than the conversion from in- to out-states, resulting in accumulation of DAT in an inward-facing conformation. It can be thought that in the time frame of the uptake and efflux experiments with mβCD, the slight difference between out-to-in and in-to-out conversion rate has no impact, and both uptake and efflux are reduced similarly (Fig. 6).

Discussion

Raft localization of DAT or direct interaction with cholesterol?

The definition of lipid rafts, or membrane rafts, has been a source of contentious debate (Pike 2006). Rafts are generally thought of as specialized microdomains comprised of sphingolipids and glycerophospholipids which facilitates the concentration of cholesterol in lipid rafts (Allen *et al.* 2007;Pike 2006). This composition makes rafts resistant to solubilization in nonionic detergents, but the concentration of detergent that should be used to define “raft-localized” DAT is not agreed on (Hong and Amara 2010;Foster *et al.* 2008;Pike 2006;Shogomori and Brown 2003). However, strong evidence for localization of a portion of DATs with membrane rafts comes from its association with other markers of rafts, such as GM1 (Foster *et al.* 2008), flotillin-1 (Cremona *et al.* 2011;Hong and Amara 2010) and syntaxin 1a (Binda *et al.* 2008). What are the differences in functionality between non-raft and raft-localized DATs? In answering this question, investigators have used the oligosaccharide mβCD as a tool to efficiently remove membrane cholesterol and thereby disrupt lipid rafts (Foster *et al.* 2008;Adkins *et al.* 2007;Zidovetzki and Levitan 2007). However, as pointed out by Hong and Amara (2010), Cremora *et al.* (2011) and by others (Zidovetzki and Levitan 2007), mβCD removes cholesterol from the membrane, reducing its content, and thereby not only disrupts lipid rafts, but also interferes with the direct interactions between cholesterol and the DAT as well as removal of specific protein regulators, extraction of phospholipids, and cytoskeletal rearrangements (Kwik *et al.* 2003;Ohvo and Slotte 1996). Thus, the reduced function in DA uptake seen with mβCD does not necessarily imply that it is caused by raft disruption. In fact, Cremona et al. (2011) show it is more likely due to the loss of a direct effect of cholesterol on the DAT, as nystatin, which disrupts rafts but maintains cholesterol in the membrane, did not affect uptake of [^{3}H]tyramine, another substrate for the DAT. In addition, depletion of flotillin-1, which is required to maintain raft-DAT, was also found not to alter [^{3}H]tyramine uptake (Cremona *et al.* 2011). Our results agree with this conclusion, as nystatin did not appreciably affect DA uptake under our conditions. To address the latter more closely, we exchanged cholesterol with desmosterol, a direct a precursor of cholesterol, which has been shown to be inefficient at replacing cholesterol in ordered membrane domains, that is, lipid rafts (Vainio *et al.* 2006;Megha *et al.* 2006). Indeed, we provide biochemical evidence to show that desmosterol repletion failed to reassemble lipid rafts as indicated by the inability to restore DAT (and flotillin-1) to lighter fractions in sucrose gradient experiments (Fig. 2). It has been shown that destabilizing lipid rafts by sterol exchange with desmosterol impaired insulin signaling, ligand binding function of the 5-HT$_{1A}$ serotonin receptor, and caveolar structure without interfering with non-raft functions of cholesterol (Singh *et al.* 2009;Jansen *et al.* 2008;Vainio *et al.* 2006;Lu *et al.* 2006;Xu *et al.* 2005;Wechsler *et al.* 2003). In comparison, DAT function as measured under the present conditions was not compromised by desmosterol repletion, but it was impacted by direct non-raft functions of cholesterol.

Given that desmosterol can be converted to cholesterol, it should be considered that this may occur within the time frame of our experiments. However, cholesterol-depleted HuH7 hepatoma cells (Vainio *et al.* 2006) or hippocampal membranes (Singh *et al.* 2009) replenished with desmosterol showed ≤10% increase in cholesterol within 1 hr. Therefore, the contribution of metabolism of desmosterol to cholesterol is likely negligible in our case. It must be noted, however, that repletion with sterols in our system resulted in ~1.5–2 fold increase over control levels (Fig. 1). We do not have the data comparing over-repletion with repletion t original starting levels and therefore more work is need to describe the changes over the entire range of cholesterol (desmosterol) levels.

Cremona *et al.* (2011) did point to the importance of raft-DAT in AMPH-induced DA efflux, based on the observed decrease in efflux upon loss of flotillin-1 in neuronal cultures.

We did not come to the same conclusion based on our efflux experiments. Besides the difference between neuronal cultures and HEK cells heterologously expressing DAT in the two studies, the efflux measurements themselves were quite different. In the present study, AMPH is used to trigger reversed transport of DA. Clearly, if changes in the uptake rate of AMPH occur by a certain experimental manipulation, it will reflect upon the efflux observed, as AMPH-induced DA efflux as measured by RDEV is primarily exchange-based (Chen *et al.* 1998). In the current work, we corrected for this by dividing the efflux V_{max} by the uptake V_{max}. It must be noted, however, that the underlying assumption is that changes in the transport rate of DA equal changes in AMPH transport. Although this is a reasonable assumption, circumstances may exist whereby transport rates for different substrates can respond differentially to a given manipulation. In order to resolve this for the present conditions, it will be required to prepare and apply [^{3}H]amphetamine, which is not currently available on the market and would have to be prepared by custom synthesis. Conversely, Cremona *et al.* (2011) monitored AMPH-induced efflux under voltage clamp, starting at a holding potential of −60 mV with subsequent stepping in 20-mV intervals in depolarizing direction. It can be seen that the difference between efflux in flotillin-1 depleted neurons and that in control neurons was not statistically significantly different below −20 mV but became increasingly so at positive potentials (+40 mV). Under our conditions, we found the membrane potential of HEK cells to be ~ −80 mV (Chen and Reith 2004), and therefore the lack of effect on AMPH-induced efflux following raft disruption (by nystatin) at this voltage agrees with the Cremona *et al.* study.

Under physiological conditions, AMPH acts on neurons going through varying membrane potentials during impulse flow. At depolarized or positive potentials, it appears that AMPH-induced efflux starts recruiting raft-DAT, as indicated by the amperometric measurements under voltage clamp (Cremona *et al.* 2011). However, at resting potential, it appears AMPH-induced efflux does not require raft-DAT, as judged from both RDEV and classical radiotracer approaches (present study). It is plausible that both mechanisms may operate differentially on DAT function dependent on whether neurons are in a resting or depolarized state (Hoffman *et al.* 1999).

Importance of conformational states of DAT in cholesterol effects

The work of Hong and Amara (2010) strongly suggests that membrane cholesterol promotes outward-facing DAT. Thus, a scenario in which cholesterol levels modulate DATs conformational equilibrium is plausible. The data presented in the last two subsections of Results on WT and W84L treated with mβCD or Zn^{2+} suggest, additionally, a mechanism by which cholesterol depletion increases the proportion of DAT in an inward-facing conformation: a slowing down of transitions between inward- and outward-facing conformations, with the conversion from out-to-in slightly less impacted than the conversion from in-to-out conversion rate. Importantly, the reduced conversion rates explain a dual effect on DA uptake and AMPH-induced DA efflux; of note, the uptake and efflux K_m and V_{max} changes observed here upon mβCD treatment of hDAT are similar to the changes described upon mutation of Thre62 to Ala in hDAT by Guptaroy *et al.* (2009). Therefore, we propose that cholesterol, by a direct action on DAT, keeps transitions between inward- and outward-facing states at equilibrium.

In this context, it is instructive to consider the steps in DA translocation: binding of DA to DAT on one side of the membrane, translocation of DA to the other side of the membrane, and DA's release. In this cycle, the return of empty carrier is the rate-limiting step in transport, which suppresses K_m to a value below the substrate binding affinity for the carrier (Erreger *et al.* 2008;Zhang *et al.* 1997). With a slower return step, K_m becomes smaller; and with a faster return step, the K_m value becomes higher-increasing towards substrate binding affinity (this can also be seen in the formulas for transport derived by us previously (Chen *et*

al. 2001;Zhang *et al.* 1997). In the presence of cholesterol (or desmosterol), the carrier returns easier when loaded with DA as speculated to occur during enhanced AMPH-induced efflux (Figs. 4B and C). If this also applies to the return of the empty carrier in a general conformational bias (Hong and Amara 2010), it would explain why cholesterol (or desmosterol) repletion has a slight tendency to increase the K_m for DA uptake (Fig. 4A). In addition to such a kinetic mechanism, another factor to consider is the effect of cholesterol in increasing the K_i of DA binding to DAT (Table 1), which also contributes to an increased uptake K_m (Fig. 4A). This K_m change agrees with the reported reduction in K_m upon cholesterol depletion with mβCD (Cremona *et al.* 2011;Adkins *et al.* 2007). In a different approach, DA affinity was assessed by competing for [^{3}H]CFT binding in whole cells and in raft-enriched fractions obtained by sucrose-density gradient separation. The IC_{50} of DA was found to be two-fold higher in rafts than whole cells (Foster *et al.* 2008). This raises the question of the importance of the distribution of surface DAT across non-raft and raft domains in the plasma membrane.

Although these data suggest a possible link between cholesterol and transporter orientation or conformational interconversion rates, other factors may be in play. DAT has been shown to exhibit channel like activity under certain conditions. In particular, Zn^{2+} has been found to facilitate amphetamine-induced substrate efflux by DAT (Scholze *et al.* 2002), subsequently shown to be due to facilitation of an uncoupled (i.e. independent of translocation of charged substrate) Cl^- transport (Meinild *et al.* 2004). It could therefore be thought that Zn^{2+} affects amphetamine-induced DA efflux in the present RDEV experiments by such an uncoupled mechanism. However, the RDEV method has been shown to primarily measure exchange-based DA efflux (Chen *et al.* 1998) and therefore uncoupling of uptake from efflux is not detected with this technique. Zn^{2+}-facilitated ion current could play a role in the present experiments on amphetamine-induced [^{3}H]DA release, but the contribution of such a mechanism appears minor as the results of these experiments were similar to those obtained with RDEV. However, the possibility that cholesterol manipulation alters DAT channel function remains intriguing and this could contribute to changes in DAT function under as yet to define conditions.

Also of note is the observed lack of effect on [^{3}H]CFT binding. Although our findings agree with Foster *et al.* (2008) in that raft-DATs displayed similar cocaine binding as whole cells, the outward-facing state of the DAT is reported to exhibit increased B_{max} of [^{3}H]CFT binding (Schmitt and Reith 2011;Hong and Amara 2010;Liang *et al.* 2009;Norregaard *et al.* 1998). Therefore, a slight increase of the inward-facing state of DAT induced by cholesterol depletion would be expected to display a reduced B_{max}, which was not seen in the present experiments (Table 1). However, for reasons not entirely understood (and discussed in (Schmitt and Reith 2011;Liang *et al.* 2009)), the effects of Zn^{2+} on the B_{max} have not been consistent between published reports. In fact, two earlier studies (Chen *et al.* 2004a;Wu *et al.* 1997) found, in the presence of Na^+, an impact of Zn^{2+} on K_d rather than B_{max}, whereas Liang *et al.* (2009) observed the B_{max} effect only in the absence of Na^+. Be that as it may, factors other than conformational changes participate in the outcome of [^{3}H]CFT binding experiments as evidenced by an unexpected lack of effect of cholesterol manipulation not only on the B_{max}, but also K_d (Table 1). This result differs from that reported by Hong and Amara (2010), and likely results from differences in the experimental conditions for measuring [^{3}H]CFT binding.

The present results along with observations by others discussed above indicate that cholesterol does play an important role in DAT function, presumably through a direct action on DAT. Evidence for cholesterol binding with integral membrane bound proteins particularly with GPCRs is mounting (Hanson *et al.* 2008). Numerous studies provide evidence of direct interactions of cholesterol with receptors and appear to be required for

structure and function (Nguyen and Taub 2003;Eroglu *et al.* 2002;Gimpl *et al.* 2000;Klein *et al.* 1995;Fernandez-Ballester *et al.* 1994). In support, studies regarding neurotransmitter proteins have suggested that cholesterol plays a direct role for optimal function although conclusive evidence is lacking (Liu *et al.* 2009;Magnani *et al.* 2004;Butchbach *et al.* 2004;Eroglu *et al.* 2002;Scanlon *et al.* 2001).

Finally, the work on cholesterol is conceptually important in linking cholesterol content of brain membranes with alterations in DAT-mediated DA neurotransmission. Given that statins are widely used to treat hypercholestemia and are amongst the most prescribed drugs in the United States, this could have major ramifications in understanding side effects of statins in relation to DA, such as symptoms of depression and cognitive impairment (Beydoun *et al.* 2011;While and Keen 2010;Kirsch *et al.* 2003). Taken together, understanding how the membrane lipid environment influences DAT function may provide important information as to one of the molecular mechanisms that participates in modulating dopaminergic activity under physiological and diseased states.

Supplementary Material

Refer to Web version on PubMed Central for supplementary material.

Acknowledgments

This work is supported by NIH T32 Grant DA007254-16, NIH Grant DA013261, NIH Grant DA019676.

Abbreviations

AMPH	dextroamphetamine
CFT	(–)-2-β-carbomethoxy-3-β-(4-fluorophenyl)tropane
DA	dopamine
hDAT	human dopamine transporter
HEK 293	human embryonic kidney cells
mβCD	methyl-β-cyclodextrin
RDEV	rotating disk electrode voltammetry
WT	wild-type

Reference List

1. Adkins EM, Samuvel DJ, Fog JU, Eriksen J, Jayanthi LD, Vaegter CB, Ramamoorthy S, Gether U. Membrane mobility and microdomain association of the dopamine transporter studied with fluorescence correlation spectroscopy and fluorescence recovery after photobleaching. Biochemistry. 2007; 46:10484–10497. [PubMed: 17711354]
2. Allen JA, Halverson-Tamboli RA, Rasenick MM. Lipid raft microdomains and neurotransmitter signalling. Nat. Rev. Neurosci. 2007; 8:128–140. [PubMed: 17195035]
3. Beydoun MA, Beason-Held LL, Kitner-Triolo MH, Beydoun HA, Ferrucci L, Resnick SM, Zonderman AB. Statins and serum cholesterol's associations with incident dementia and mild cognitive impairment. J. Epidemiol. Community Health. 2011; 65:949–957. [PubMed: 20841372]
4. Binda F, Dipace C, Bowton E, Robertson SD, Lute BJ, Fog JU, Zhang M, Sen N, Colbran RJ, Gnegy ME, Gether U, Javitch JA, Erreger K, Galli A. Syntaxin 1A interaction with the dopamine transporter promotes amphetamine-induced dopamine efflux. Mol. Pharmacol. 2008; 74:1101–1108. [PubMed: 18617632]

5. Bjorklund NL, Volz TJ, Schenk JO. Differential effects of Zn2+ on the kinetics and cocaine inhibition of dopamine transport by the human and rat dopamine transporters. Eur. J. Pharmacol. 2007; 565:17–25. [PubMed: 17408612]
6. Bonisch H. Transport and drug binding kinetics in membrane vesicle preparation. Methods Enzymol. 1998; 296:259–278. 259–278. [PubMed: 9779454]
7. Butchbach ME, Tian G, Guo H, Lin CL. Association of excitatory amino acid transporters, especially EAAT2, with cholesterol-rich lipid raft microdomains: importance for excitatory amino acid transporter localization and function. J. Biol. Chem. 2004; 279:34388–34396. [PubMed: 15187084]
8. Chen N, Justice JB. Differential effect of structural modification of human dopamine transporter on the inward and outward transport of dopamine. Brain Res. Mol. Brain Res. 2000; 75:208–215. [PubMed: 10686341]
9. Chen N, Reith ME. Na+ and the substrate permeation pathway in dopamine transporters. Eur. J. Pharmacol. 2003; 479:213–221. [PubMed: 14612151]
10. Chen N, Reith ME. Interaction between dopamine and its transporter: role of intracellular sodium ions and membrane potential. J. Neurochem. 2004; 89:750–765. [PubMed: 15086531]
11. Chen N, Rickey J, Berfield JL, Reith MEA. Aspartate 345 of the dopamine transporter is critical for conformational changes in substrate translocation and cocaine binding. J. Biol. Chem. 2004a; 279:5508–5519. [PubMed: 14660644]
12. Chen N, Trowbridge CG, Justice JBJ. Voltammetric studies on mechanisms of dopamine efflux in the presence of substrates and cocaine from cells expressing human norepinephrine transporter. J. Neurochem. 1998; 71:653–665. [PubMed: 9681456]
13. Chen N, Vaughan RA, Reith ME. The role of conserved tryptophan and acidic residues in the human dopamine transporter as characterized by site-directed mutagenesis. J. Neurochem. 2001; 77:1116–1127. [PubMed: 11359877]
14. Chen N, Zhen J, Reith MEA. Mutation of Trp84 and Asp313 of the dopamine transporter reveals similar mode of binding interaction for GBR 12909 and benztropine as opposed to cocaine. J. Neurochem. 2004b; 89:853–864. [PubMed: 15140185]
15. Christian AE, Haynes MP, Phillips MC, Rothblat GH. Use of cyclodextrins for manipulating cellular cholesterol content. J. Lipid Res. 1997; 38:2264–2272. [PubMed: 9392424]
16. Cremona ML, Matthies HJ, Pau K, Bowton E, Speed N, Lute BJ, Anderson M, Sen N, Robertson SD, Vaughan RA, Rothman JE, Galli A, Javitch JA, Yamamoto A. Flotillin-1 is essential for PKC-triggered endocytosis and membrane microdomain localization of DAT. Nat. Neurosci. 2011; 14:469–477. [PubMed: 21399631]
17. Dietz DM, Dietz KC, Nestler EJ, Russo SJ. Molecular mechanisms of psychostimulant-induced structural plasticity. Pharmacopsychiatry. 2009; 42(Suppl 1):S69–S78. [PubMed: 19434558]
18. Eroglu C, Cronet P, Panneels V, Beaufils P, Sinning I. Functional reconstitution of purified metabotropic glutamate receptor expressed in the fly eye. EMBO Rep. 2002; 3:491–496. [PubMed: 11964379]
19. Erreger K, Grewer C, Javitch JA, Galli A. Currents in response to rapid concentration jumps of amphetamine uncover novel aspects of human dopamine transporter function. J. Neurosci. 2008; 28:976–989. [PubMed: 18216205]
20. Falkenburger BH, Barstow KL, Mintz IM. Dendrodendritic inhibition through reversal of dopamine transport. Science. 2001; 293:2465–2470. [PubMed: 11577238]
21. Fernandez-Ballester G, Castresana J, Fernandez AM, Arrondo JL, Ferragut JA, Gonzalez-Ros JM. A role for cholesterol as a structural effector of the nicotinic acetylcholine receptor. Biochemistry. 1994; 33:4065–4071. [PubMed: 8142409]
22. Foster JD, Adkins SD, Lever JR, Vaughan RA. Phorbol ester induced trafficking-independent regulation and enhanced phosphorylation of the dopamine transporter associated with membrane rafts and cholesterol. J. Neurochem. 2008; 105:1683–1699. [PubMed: 18248623]
23. Gimpl G, Burger K, Politowska E, Ciarkowski J, Fahrenholz F. Oxytocin receptors and cholesterol: interaction and regulation. Exp. Physiol. 2000; 85(Spec No):41S–49S. [PubMed: 10795905]

24. Gnegy ME. The effect of phosphorylation on amphetamine-mediated outward transport. Eur. J. Pharmacol. 2003; 479:83–91. [PubMed: 14612140]
25. Guptaroy B, Zhang M, Bowton E, Binda F, Shi L, Weinstein H, Galli A, Javitch JA, Neubig RR, Gnegy ME. A juxtamembrane mutation in the N terminus of the dopamine transporter induces preference for an inward-facing conformation. Mol. Pharmacol. 2009; 75:514–524. [PubMed: 19098122]
26. Hanson MA, Cherezov V, Griffith MT, Roth CB, Jaakola VP, Chien EY, Velasquez J, Kuhn P, Stevens RC. A specific cholesterol binding site is established by the 2.8 A structure of the human beta2-adrenergic receptor. Structure. 2008; 16:897–905. [PubMed: 18547522]
27. Hoffman AF, Zahniser NR, Lupica CR, Gerhardt GA. Voltage-dependency of the dopamine transporter in the rat substantia nigra. Neurosci. Lett. 1999; 260:105–108. [PubMed: 10025710]
28. Hong WC, Amara SG. Membrane cholesterol modulates the outward-facing conformation of the dopamine transporter and alters cocaine binding. J. Biol. Chem. 2010
29. Jansen M, Pietiainen VM, Polonen H, Rasilainen L, Koivusalo M, Ruotsalainen U, Jokitalo E, Ikonen E. Cholesterol substitution increases the structural heterogeneity of caveolae. J. Biol. Chem. 2008; 283:14610–14618. [PubMed: 18353778]
30. Jayanthi LD, Samuvel DJ, Ramamoorthy S. Regulated internalization and phosphorylation of the native norepinephrine transporter in response to phorbol esters. Evidence for localization in lipid rafts and lipid raft-mediated internalization. J. Biol. Chem. 2004; 279:19315–19326. [PubMed: 14976208]
31. Kirsch C, Eckert GP, Mueller WE. Statin effects on cholesterol micro-domains in brain plasma membranes. Biochem. Pharmacol. 2003; 65:843–856. [PubMed: 12628479]
32. Klein U, Gimpl G, Fahrenholz F. Alteration of the myometrial plasma membrane cholesterol content with beta-cyclodextrin modulates the binding affinity of the oxytocin receptor. Biochemistry. 1995; 34:13784–13793. [PubMed: 7577971]
33. Kurian MA, Li Y, Zhen J, Meyer E, Hai N, Christen HJ, Hoffmann GF, Jardine P, von MA, Mordekar SR, O'Callaghan F, Wassmer E, Wraige E, Dietrich C, Lewis T, Hyland K, Heales S Jr, Sanger T, Gissen P, Assmann BE, Reith ME, Maher ER. Clinical and molecular characterisation of hereditary dopamine transporter deficiency syndrome: an observational cohort and experimental study. Lancet Neurol. 2011; 10:54–62. [PubMed: 21112253]
34. Kwik J, Boyle S, Fooksman D, Margolis L, Sheetz MP, Edidin M. Membrane cholesterol, lateral mobility, and the phosphatidylinositol 4,5-bisphosphate-dependent organization of cell actin. Proc. Natl. Acad. Sci. U. S. A. 2003; 100:13964–13969. [PubMed: 14612561]
35. Leviel V. Dopamine release mediated by the dopamine transporter, facts and consequences. J. Neurochem. 2011
36. Liang YJ, Zhen J, Chen N, Reith ME. Interaction of catechol and non-catechol substrates with externally or internally facing dopamine transporters. J. Neurochem. 2009; 109:981–994. [PubMed: 19519772]
37. Liu X, Mitrovic AD, Vandenberg RJ. Glycine transporter 1 associates with cholesterol-rich membrane raft microdomains. Biochem. Biophys. Res. Commun. 2009; 384:530–534. [PubMed: 19427831]
38. Loland CJ, Granas C, Javitch JA, Gether U. Identification of intracellular residues in the dopamine transporter critical for regulation of transporter conformation and cocaine binding. J. Biol. Chem. 2004; 279:3228–3238. [PubMed: 14597628]
39. Loland CJ, Norregaard L, Litman T, Gether U. Generation of an activating Zn(2+) switch in the dopamine transporter: mutation of an intracellular tyrosine constitutively alters the conformational equilibrium of the transport cycle. Proc. Natl. Acad. Sci. U. S. A. 2002; 99:1683–1688. [PubMed: 11818545]
40. Lu X, Kambe F, Cao X, Yoshida T, Ohmori S, Murakami K, Kaji T, Ishii T, Zadworny D, Seo H. DHCR24-knockout embryonic fibroblasts are susceptible to serum withdrawal-induced apoptosis because of dysfunction of caveolae and insulin-Akt-Bad signaling. Endocrinology. 2006; 147:3123–3132. [PubMed: 16513830]

41. Magnani F, Tate CG, Wynne S, Williams C, Haase J. Partitioning of the serotonin transporter into lipid microdomains modulates transport of serotonin. J. Biol. Chem. 2004; 279:38770–38778. [PubMed: 15226315]
42. Megha, Bakht O, London E. Cholesterol precursors stabilize ordinary and ceramide-rich ordered lipid domains (lipid rafts) to different degrees. Implications for the Bloch hypothesis and sterol biosynthesis disorders. J. Biol. Chem. 2006; 281:21903–21913. [PubMed: 16735517]
43. Meinild AK, Sitte HH, Gether U. Zinc potentiates an uncoupled anion conductance associated with the dopamine transporter. J. Biol. Chem. 2004; 279:49671–49679. [PubMed: 15358780]
44. Nguyen DH, Taub DD. Inhibition of chemokine receptor function by membrane cholesterol oxidation. Exp. Cell Res. 2003; 291:36–45. [PubMed: 14597406]
45. Norregaard L, Frederiksen D, Nielsen EO, Gether U. Delineation of an endogenous zinc-binding site in the human dopamine transporter. EMBO J. 1998; 17:4266–4273. [PubMed: 9687495]
46. Ohvo H, Slotte JP. Cyclodextrin-mediated removal of sterols from monolayers: effects of sterol structure and phospholipids on desorption rate. Biochemistry. 1996; 35:8018–8024. [PubMed: 8672506]
47. Olivier V, Guibert B, Leviel V. Direct in vivo comparison of two mechanisms releasing dopamine in the rat striatum. Brain Res. 1995; 695:1–9. [PubMed: 8574640]
48. Patterson TA, Brot MD, Zavosh A, Schenk JO, Szot P, Figlewicz DP. Food deprivation decreases mRNA and activity of the rat dopamine transporter. Neuroendocrinology. 1998; 68:11–20. [PubMed: 9695934]
49. Pike LJ. Rafts defined: a report on the Keystone Symposium on Lipid Rafts and Cell Function. J. Lipid Res. 2006; 47:1597–1598. [PubMed: 16645198]
50. Pucadyil TJ, Shrivastava S, Chattopadhyay A. The sterol-binding antibiotic nystatin differentially modulates ligand binding of the bovine hippocampal serotonin1A receptor. Biochem. Biophys. Res. Commun. 2004; 320:557–562. [PubMed: 15219865]
51. Rice ME, Cragg SJ. Dopamine spillover after quantal release: rethinking dopamine transmission in the nigrostriatal pathway 1. Brain Res. Rev. 2008; 58:303–313. [PubMed: 18433875]
52. Rothberg KG, Ying YS, Kamen BA, Anderson RG. Cholesterol controls the clustering of the glycophospholipid-anchored membrane receptor for 5-methyltetrahydrofolate. J. Cell Biol. 1990; 111:2931–2938. [PubMed: 2148564]
53. Rothman RB, Dersch CM, Ananthan S, Partilla JS. Studies of the biogenic amine transporters. 13. Identification of "agonist" and "antagonist" allosteric modulators of amphetamine-induced dopamine release. J. Pharmacol. Exp. Ther. 2009; 329:718–728. [PubMed: 19244097]
54. Russo SJ, Dietz DM, Dumitriu D, Morrison JH, Malenka RC, Nestler EJ. The addicted synapse: mechanisms of synaptic and structural plasticity in nucleus accumbens. Trends Neurosci. 2010; 33:267–276. [PubMed: 20207024]
55. Scanlon SM, Williams DC, Schloss P. Membrane cholesterol modulates serotonin transporter activity. Biochemistry. 2001; 40:10507–10513. [PubMed: 11523992]
56. Schmitt KC, Reith ME. The atypical stimulant and nootropic modafinil interacts with the dopamine transporter in a different manner than classical cocaine-like inhibitors. PLoS. One. 2011; 6:e25790. [PubMed: 22043293]
57. Schmitt KC, Zhen J, Kharkar P, Mishra M, Chen N, Dutta AK, Reith ME. Interaction of cocaine-, benztropine-, and GBR12909-like compounds with wild-type and mutant human dopamine transporters: molecular features that differentially determine antagonist-binding properties. J. Neurochem. 2008; 107:928–940. [PubMed: 18786172]
58. Schoffelmeer AN, Drukarch B, De Vries TJ, Hogenboom F, Schetters D, Pattij T. Insulin modulates cocaine-sensitive monoamine transporter function and impulsive behavior. J. Neurosci. 2011; 31:1284–1291. [PubMed: 21273413]
59. Scholze P, Norregaard L, Singer EA, Freissmuth M, Gether U, Sitte HH. The role of zinc ions in reverse transport mediated by monoamine transporters. J. Biol. Chem. 2002; 277:21505–21513. [PubMed: 11940571]
60. Shogomori H, Brown DA. Use of detergents to study membrane rafts: the good, the bad the ugly. Biol. Chem. 2003; 384:1259–1263. [PubMed: 14515986]

61. Simons K, Toomre D. Lipid rafts and signal transduction. Nat. Rev. Mol. Cell Biol. 2000; 1:31–39. [PubMed: 11413487]
62. Singh P, Saxena R, Paila YD, Jafurulla M, Chattopadhyay A. Differential effects of cholesterol and desmosterol on the ligand binding function of the hippocampal serotonin (1A) receptor: implications in desmosterolosis. Biochim. Biophys. Acta. 2009; 1788:2169–2173. [PubMed: 19616511]
63. Sitte HH, Huck S, Reither H, Boehm S, Singer EA, Pifl C. Carrier-mediated release, transport rates, and charge transfer induced by amphetamine, tyramine, and dopamine in mammalian cells transfected with the human dopamine transporter. J. Neurochem. 1998; 71:1289–1297. [PubMed: 9721755]
64. Sorkina T, Hoover BR, Zahniser NR, Sorkin A. Constitutive and Protein Kinase C-Induced Internalization of the Dopamine Transporter is Mediated by a Clathrin-Dependent Mechanism. Traffic. 2005; 6:157–170. [PubMed: 15634215]
65. Speed N, Saunders C, Davis AR, Owens WA, Matthies HJ, Saadat S, Kennedy JP, Vaughan RA, Neve RL, Lindsley CW, Russo SJ, Daws LC, Niswender1 KD, Galli A. Impaired Striatal Akt Signaling Disrupts Dopamine Homeostasis and Increases Feeding. PLoS. One. 2011; 6:e25169. [PubMed: 21969871]
66. Stevenson J, Brown AJ. How essential is cholesterol? Biochem. J. 2009; 420:e1–e4. [PubMed: 19426142]
67. Sulzer D. How addictive drugs disrupt presynaptic dopamine neurotransmission. Neuron. 2011; 69:628–649. [PubMed: 21338876]
68. Sulzer D, Sonders MS, Poulsen NW, Galli A. Mechanisms of neurotransmitter release by amphetamines: a review. Prog. Neurobiol. 2005; 75:406–433. [PubMed: 15955613]
69. Vainio S, Jansen M, Koivusalo M, Rog T, Karttunen M, Vattulainen I, Ikonen E. Significance of sterol structural specificity. Desmosterol cannot replace cholesterol in lipid rafts. J. Biol. Chem. 2006; 281:348–355. [PubMed: 16249181]
70. Wall SC, Gu H, Rudnick G. Biogenic amine flux mediated by cloned transporters stably expressed in cultured cell lines: amphetamine specificity for inhibition and efflux. Mol. Pharmacol. 1995; 47:544–550. [PubMed: 7700252]
71. Wechsler A, Brafman A, Shafir M, Heverin M, Gottlieb H, Damari G, Gozlan-Kelner S, Spivak I, Moshkin O, Fridman E, Becker Y, Skaliter R, Einat P, Faerman A, Bjorkhem I, Feinstein E. Generation of viable cholesterol-free mice. Science. 2003; 302:2087. [PubMed: 14684813]
72. While A, Keen L. The effects of statins on mood: A review of the literature. Eur. J. Cardiovasc. Nurs. 2010
73. Wu Q, Coffey LL, Reith ME. Cations affect [3H]mazindol and [3H]WIN 35,428 binding to the human dopamine transporter in a similar fashion. J. Neurochem. 1997; 69:1106–1118. [PubMed: 9282933]
74. Xu F, Rychnovsky SD, Belani JD, Hobbs HH, Cohen JC, Rawson RB. Dual roles for cholesterol in mammalian cells. Proc. Natl. Acad. Sci. U. S. A. 2005; 102:14551–14556. [PubMed: 16199524]
75. Zhang L, Coffey LL, Reith ME. Regulation of the functional activity of the human dopamine transporter by protein kinase C. Biochem. Pharmacol. 1997; 53:677–688. [PubMed: 9113087]
76. Zhen J, Reith ME, Carr KD. Chronic food restriction and dopamine transporter function in rat striatum. Brain Res. 2006; 1082:98–101. [PubMed: 16516172]
77. Zidovetzki R, Levitan I. Use of cyclodextrins to manipulate plasma membrane cholesterol content: evidence, misconceptions and control strategies. Biochim. Biophys. Acta. 2007; 1768:1311–1324. [PubMed: 17493580]

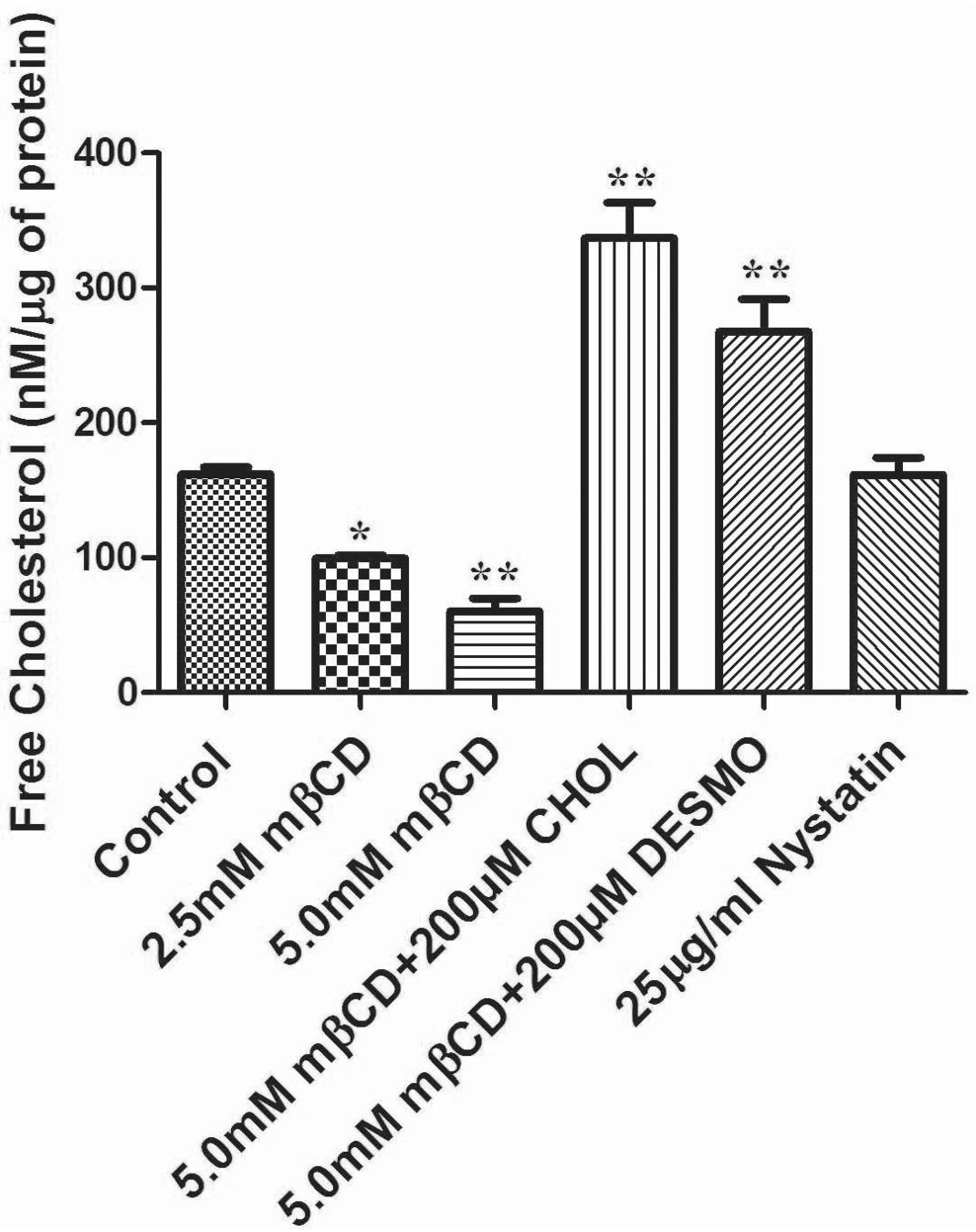

Figure 1.

Effects of cholesterol manipulation on total levels of unesterified cholesterol in HEK 293-hDAT cells. Values are mean ± SE for 5–10 independent experiments measured in duplicate ** $P<0.001$, * $P<0.05$ (compared with Control, one-way ANOVA followed by Dunnett multiple comparions test.

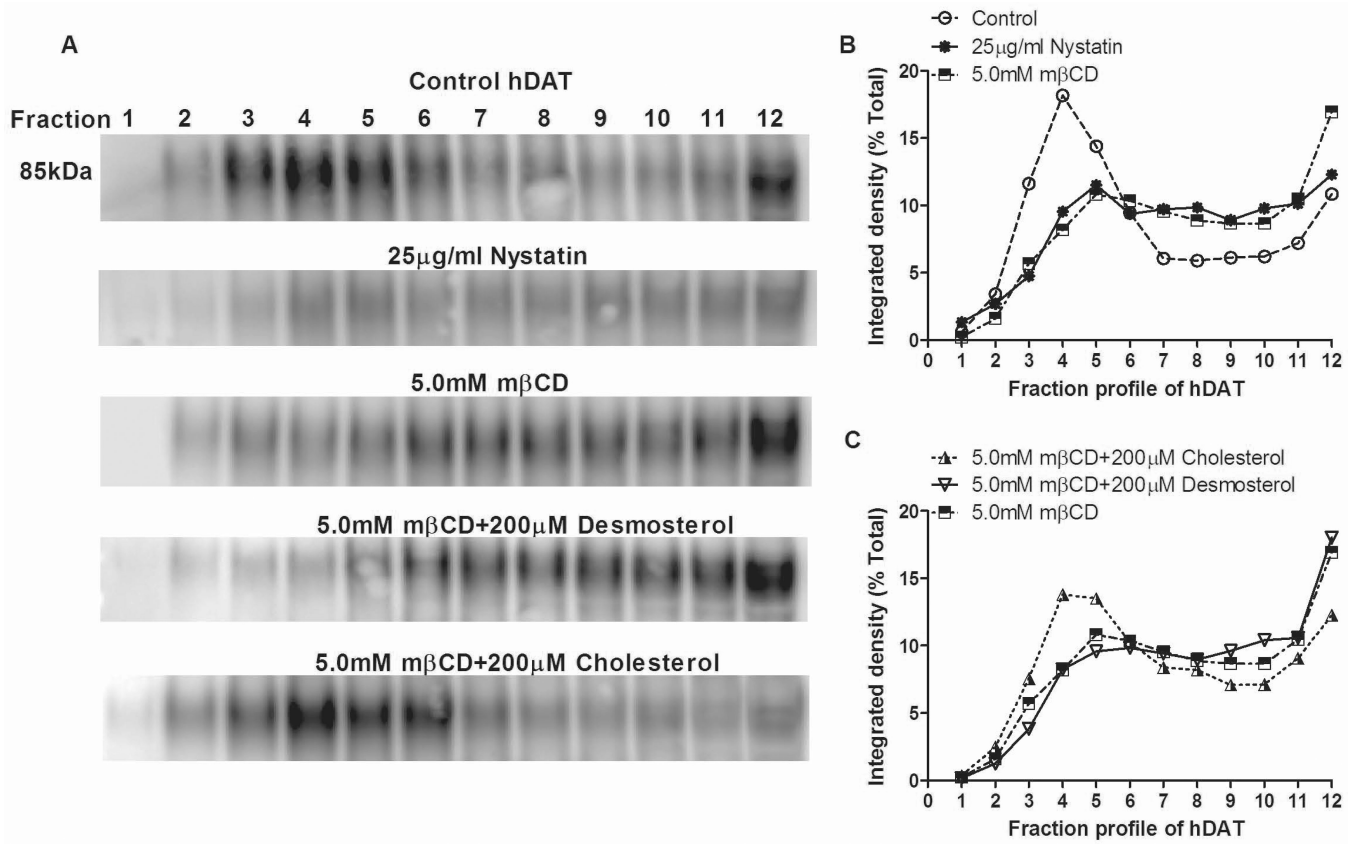

Figure 2.

Effects of lipid raft-destabalizing agents and sterol repletion on DAT association with lipid rafts. Treated HEK-293 hDAT cells were solubilized in 1% Brij and subjected to discontinuous sucrose density centrifugation. Twelve fractions of equal volumes were collected from top (Fraction 1) to bottom (Fraction 12). Each fraction was processed for SDS-PAGE and subjected to immunoblotting for hDAT (shown), flotillin-1, and TfR (Supplementary Information). Shown are representative blots (A) and quantification of DAT distribution across gradients (n=3–5) (B and C). Data for each fraction are expressed as mean of band intensities as a percentage of the sum total for DAT protein found within all fractions. The average SE (not shown) was 12 %.

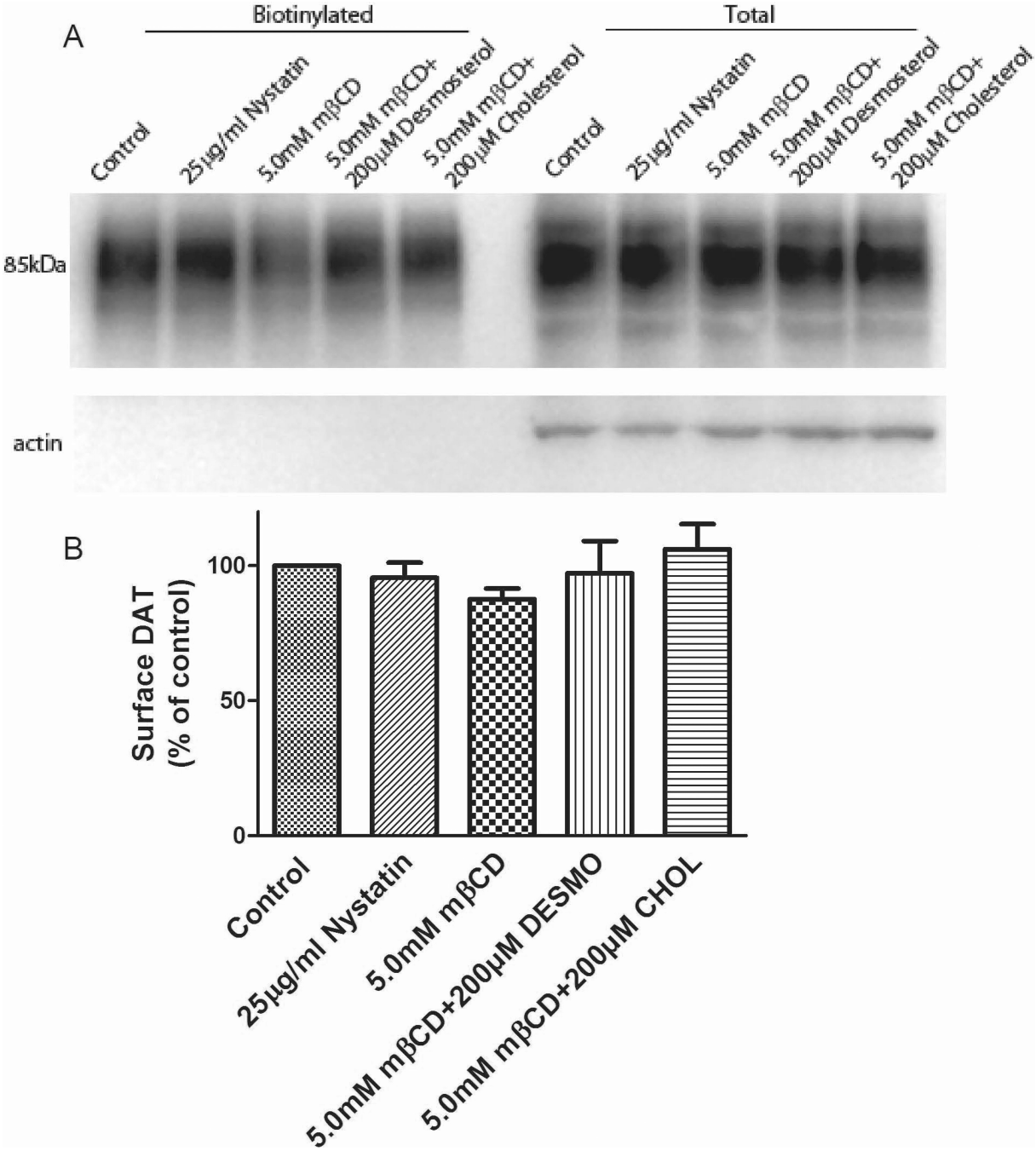

Figure 3.

Surface expression levels of hDAT stably expressed in HEK-293 cells in response to changes in membrane cholesterol. (A) Representative immunoblot showing biotinylated (surface DAT) and total extracts after treatments. (B) Quantification of surface DAT after treatments expressed as percentage of control (means ± SE of four independent experiments).

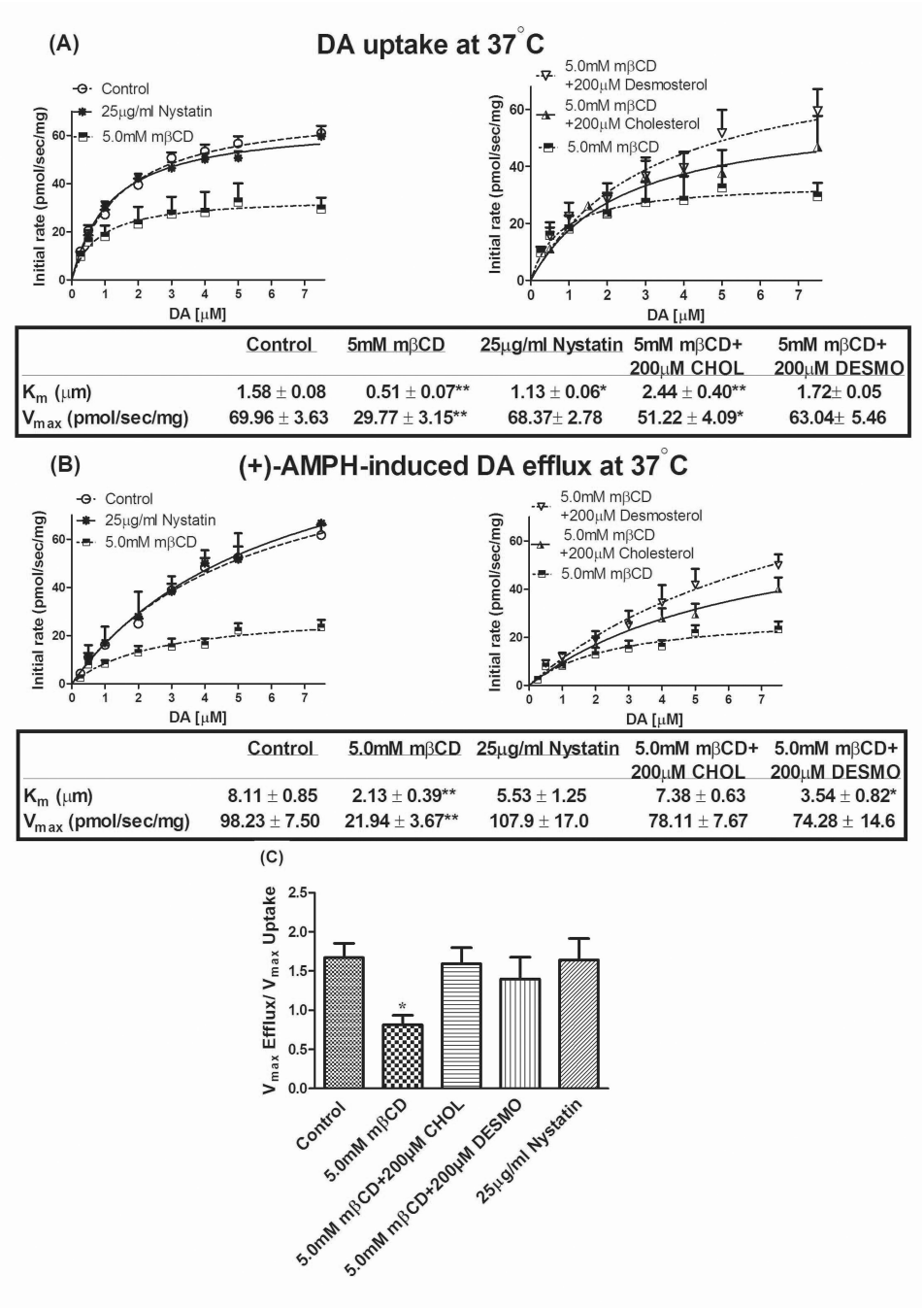

	Control	5mM mβCD	25μg/ml Nystatin	5mM mβCD+ 200μM CHOL	5mM mβCD+ 200μM DESMO
K_m (μm)	1.58 ± 0.08	0.51 ± 0.07**	1.13 ± 0.06*	2.44 ± 0.40**	1.72± 0.05
V_{max} (pmol/sec/mg)	69.96 ± 3.63	29.77 ± 3.15**	68.37± 2.78	51.22 ± 4.09*	63.04± 5.46

	Control	5.0mM mβCD	25μg/ml Nystatin	5.0mM mβCD+ 200μM CHOL	5.0mM mβCD+ 200μM DESMO
K_m (μm)	8.11 ± 0.85	2.13 ± 0.39**	5.53 ± 1.25	7.38 ± 0.63	3.54 ± 0.82*
V_{max} (pmol/sec/mg)	98.23 ± 7.50	21.94 ± 3.67**	107.9 ± 17.0	78.11 ± 7.67	74.28 ± 14.6

Figure 4.

Effect of cholesterol manipulation on (A) DA uptake and (B) AMPH-induced DA efflux at various concentrations of DA measured with RDEV at 37°C in the same cell suspension. Panel (C) shows the ratio of DA uptake and efflux V_{max} (corrected efflux V_{max}) calculated for each independent experiment. HEK 293-hDAT cells were treated with 5.0 mM mβCD or 25 μg/ml nystatin at 37°C for 30 min and 45 min, respectively. To restore cholesterol or desmosterol levels, both were pre-complexed with mβCD in serum free DMEM and incubated for an additional 2 hrs. Vehicle and 5.0 mM mβCD treated cells were incubated for 2 hrs in serum free DMEM as matched controls. Cells suspended in KRH buffer (with or without nystatin) were exposed to DA followed by addition of 10 μM of AMPH. Solid lines

are fits to the Michaelis-Menten model for the averaged data for each separate DA concentration as part of the DA concentration curve. Kinetic constants were calculated using Kell Radlig and represented as mean ± SE for 6–12 independent experiments. $^{**}P<0.001$, $^{*}P<0.05$ (compared with Control, one-way ANOVA followed by Dunnett multiple comparisons test).

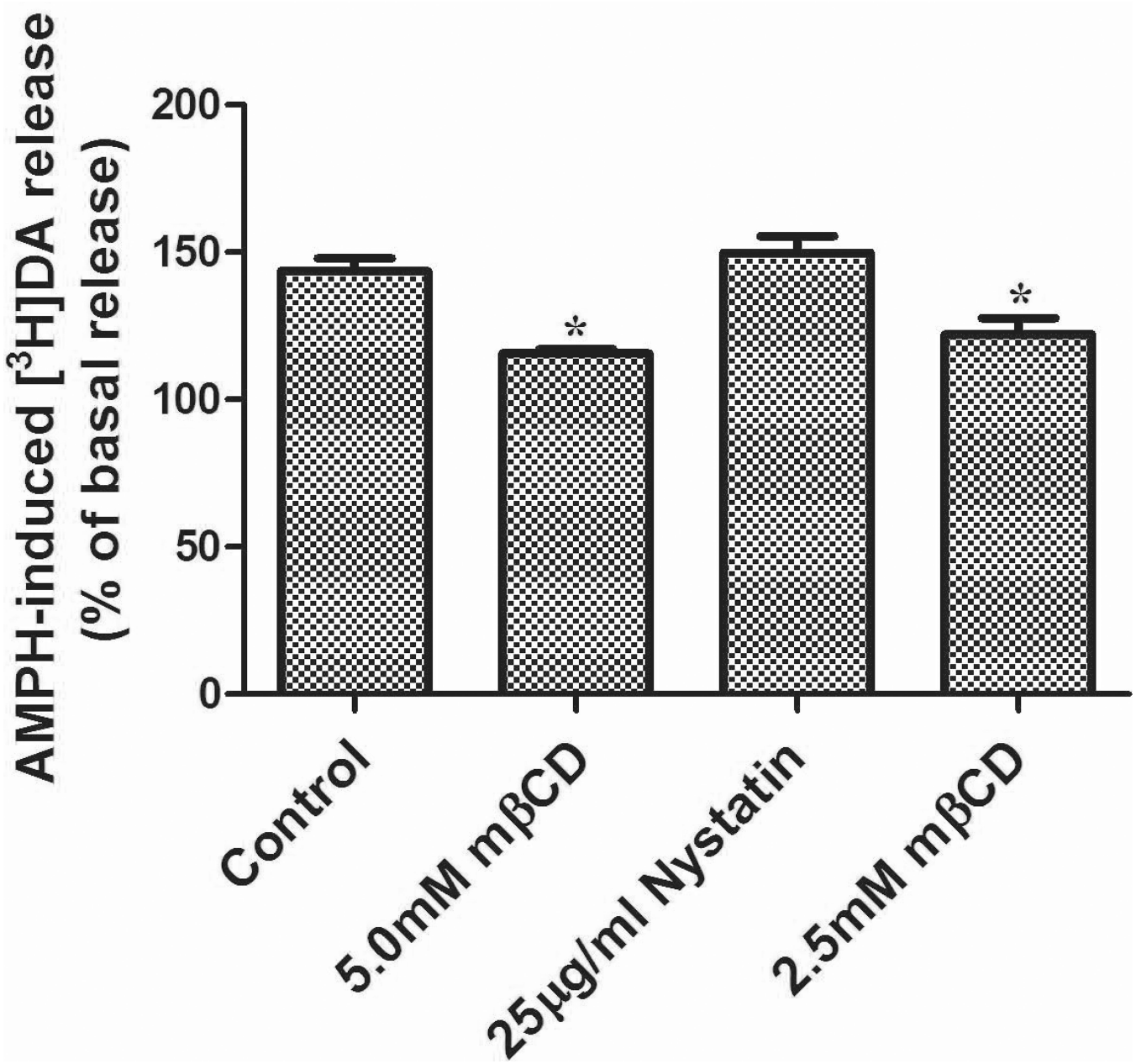

Figure 5.

LLC-PK-hDAT cells were pretreated with vehicle or compounds for 20 min at 37 °C in KRH buffer followed by [^{3}H]DA (10 nM) for an additional 20 min at 37°C. Washed cells were treated with or without 10 μM AMPH and after 5 min, aliquots of supernatant were taken to assess [^{3}H]DA release. Data are mean ± SE, n=4. *P<0.05 (compared with Control, one-way ANOVA followed by Dunnett multiple comparisons test).

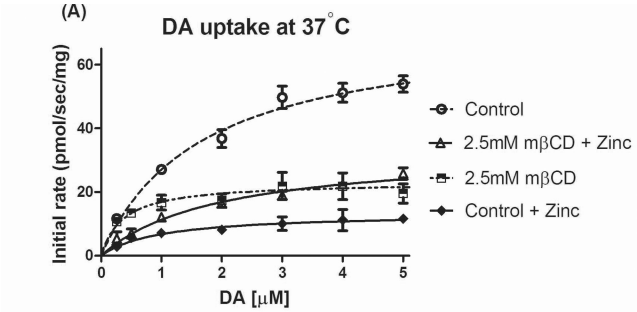

	Control	2.5mM mβCD	30μM Zinc	2.5mM mβCD+ 30μM Zinc
K_m (μm)	1.45 ± 0.10	0.54 ± 0.13*	0.89 ± 0.24	1.58 ± 0.34^{++}
V_{max} (pmol/sec/mg)	53.25 ± 2.93	22.12 ± 2.80*	11.95 ± 1.19*$^{+}$	29.73 ± 3.57*$^{\#}$

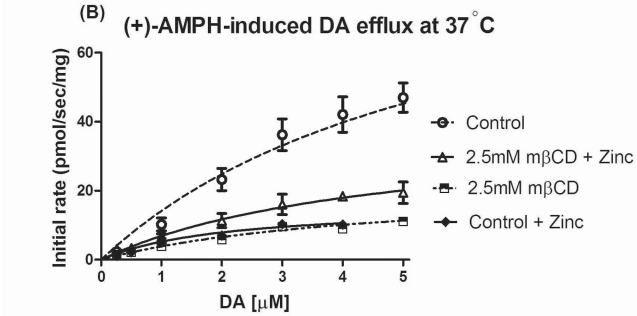

	Control	2.5mM mβCD	30μM Zinc	2.5mM mβCD+ 30μM Zinc
K_m (μm)	8.35 ± 0.68	4.39 ± 0.60*	1.74 ± 0.41**$^{+}$	6.19 ± 1.17$^{\#}$
V_{max} (pmol/sec/mg)	97.6 ± 7.77	21.64 ± 2.71**	20.25 ± 4.38**	50.31 ± 5.33*$^{\#++}$

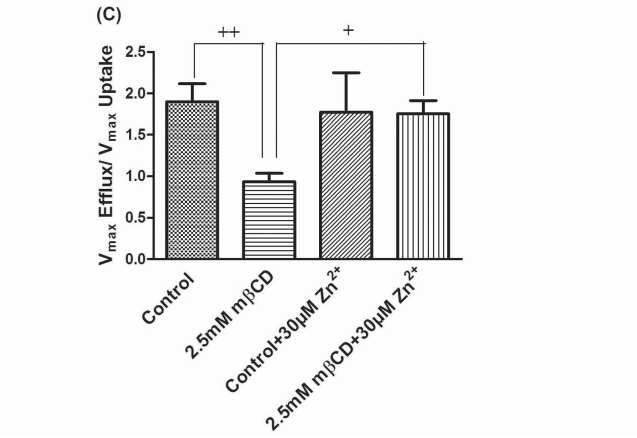

Figure 6.

Effects of zinc on DAT uptake (A) and efflux (B) at various concentrations of DA measured with RDEV at 37°C in the same cell suspension. Panel (C) shows the ratio of DA uptake and efflux (corrected efflux V_{max}) calculated for each independent experiment. HEK 293-hDAT cells were treated with 2.5mM mβCD at 37°C for 30min. Cells were then pretreated with 30 μM Zn^{2+} for 1 minute prior to DA addition followed by 10 μM of AMPH. Data are presented for 4–10 independent experiments, and otherwise details are as in Fig. 4. Panel A; *P<0.001 (vs. Control), ^{+}P<0.05 and ^{++}P<0.01 (vs. mβCD), $^{\#}P$<0.001 (vs. Zn^{2+}); Panel B: *P<0.01 and **P<0.001 (vs. Control), ^{+}P<0.01 and ^{++}P<0.001 (vs. mβCD), $^{\#}P$<0.001 (vs.

Zn^{2+}); Panel C: $^{+}P<0.05$ and $^{++}P<0.01$ (vs. mβCD) (one-way ANOVA followed by Tukey-Kramer multiple comparisons test).

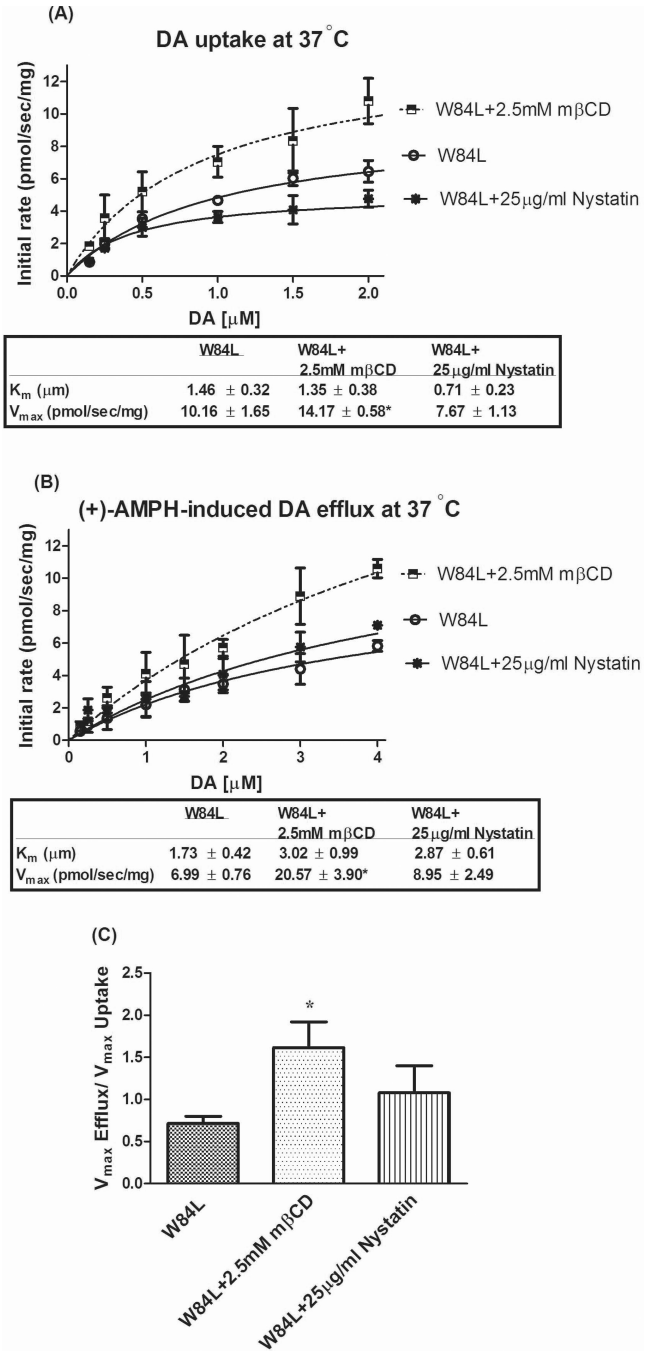

	W84L	W84L+ 2.5mM mβCD	W84L+ 25μg/ml Nystatin
K_m (μm)	1.46 ± 0.32	1.35 ± 0.38	0.71 ± 0.23
V_{max} (pmol/sec/mg)	10.16 ± 1.65	14.17 ± 0.58*	7.67 ± 1.13

	W84L	W84L+ 2.5mM mβCD	W84L+ 25μg/ml Nystatin
K_m (μm)	1.73 ± 0.42	3.02 ± 0.99	2.87 ± 0.61
V_{max} (pmol/sec/mg)	6.99 ± 0.76	20.57 ± 3.90*	8.95 ± 2.49

Figure 7.

Effects of cholesterol removal or chelation on W84L uptake (A) and efflux (B) at various concentrations of DA measured with RDEV at 37°C in the same cell suspension. Panel (C) shows the ratio of DA uptake and efflux (corrected efflux V_{max}) calculated for each independent experiment. W84L hDAT-HEK 293 cells were treated with 2.5mM mβCD or 25 μg/ml nystatin at 37°C for 30 min and 45 min, respectively. These cells were then exposed to DA followed by 10 μM of AMPH. Data are presented for 6–8 independent experiments, and otherwise details are as in Fig. 4. **P*<0.05 (compared with W84L, one-way ANOVA followed by Dunnett multiple comparisons test).

Table 1

Effect of cholesterol reduction and replenishment in intact HEK 293-hDAT cells

	[^{3}H]DA Uptake		[^{3}H]CFT Binding		Competition for [^{3}H]CFT binding by DA
	K_m (μM)	V_{max} (pmol/mg/min)	K_d (nM)	B_{max} (pmol/mg)	K_i for Dopamine (μM)
Control	0.40±0.05	4.28±0.74	15.6±1.97	3.68±0.46	3.47±0.60
5.0mM mβCD	0.17±0.03 *	1.84±0.35 *	17.80±2.17	3.07±0.57	2.18±0.22 *
5.0mM mβCD + 200 μM CHOL	0.49±0.06	2.87±0.65	14.62±2.07	3.98 ±0.62	4.05±0.51

Cells were first pretreated with vehicle or 5.0 mM mβCD in SF-DMEM for 30 min at 37°C. To restore cholesterol levels, cholesterol was pre-complexed mβCD at a ratio of 12.5:1 and incubated for an additional 2 hrs in SF-DMEM. Treated cells were subsequently incubated at 25°C with either 10 nM [^{3}H]DA for 5 min (uptake assays) or 4 nM [^{3}H]CFT for 15 min (binding assays) in modified KRH buffer, with or without 5.0 mM mβCD. Values represent mean ± SE of 5 or more experiments, each performed across triplicate wells.

* $P < 0.05$ compared with control (ANOVA, Dunnett multiple-comparisons test).

Table 2

Effect of cholesterol reduction in intact HEK cells expressing WT or W84L hDAT

	[^{3}H]DA Uptake		[^{3}H]CFT Binding		Competition for [^{3}H]CFT binding by DA
	K_m (μM)	V_{max} (pmol/mg/min)	K_d (nM)	B_{max} (pmol/mg)	K_i for Dopamine (μM)
WT DAT	0.40±0.05	4.28±0.74	15.6±1.97	3.68±0.46	3.47±0.60
W84L	0.34±0.13	1.95±0.44 *	2.58±0.46 *	4.77±0.85	9.77±1.88 *
W84L + mβCD	0.37±0.11	3.03±0.75	2.38±0.29 *	4.42±0.73	4.34±1.42

Cells were first pretreated with vehicle or 2.5 mM mβCD in SF-DMEM for 30 min at 37°C. Following pretreatment, cells were subsequently incubated at 25°C with either 10 nM [^{3}H]DA for 5 min (uptake assays) or 4 nM [^{3}H]CFT for 15 min (binding assays) in modified KRH buffer, with or without 2.5mM mβCD. Values represent mean ± SE of 5 or more experiments, each performed across triplicate wells.

* $P < 0.05$ compared with control (ANOVA, Dunnett multiple-comparisons test).